Multiple Element Antenna Placement and Structure Studies in Subway Environments.

J. A. Valdesueiro†, B. Izquierdo, J. Romeu
†AntennaLAB, Department of Signal Theory and Communications, Universitat Politècnica de Catalunya
Jordi Girona 1-3, Barcelona, Spain
javalde@tsc.upc.edu

***Abstract*—Public subway transport networks require reliable high data reate wireless communication systems. One way to increase the maximum theoretical capacity in a certain environment is to apply the known MIMO techniques in order to maximize the presence of orthogonal sub-channels in a certain radio-channel. In this work the authors present a method to assess the impact of the position inside the tunnel and the diversity configuration of the antennas of the considered MIMO system on the maximum theoretical capacity of the radio-channel inside subway tunnels.**

I. Introduction

Recent projects on communication systems working at subway and train environments have included a high data rate wireless communication network deployment in their designs. This need has triggered the research studies on how to model the propagation in train tunnels [1], [2], [3], [4], [5], [6].

In this work the authors study the impact on the maximum theoretical capacity of the array position inside the tunnel and the polarization diversity technique when a 2 transmitting and 2 receiving elements structure is considered. This analysis is based on the modal decomposition of the electrical field inside tunnels presented at [7], [8] and [9], and the propagation in the spectral domain presented at [10] and [11].

A quasi-static radio-propagation channel is assumed with a sampled channel matrix $\hat{H}$ for a MxM MIMO system. This channel matrix is computed for different antenna position and orientation as a function of the distance between thransmitter and receiver. Two canonical tunnel cross-section are considered: reactangular and circular (see Fig. 1).

Once the matrix $\hat{H}$ is obtained, the channel correlation matrix at the receiver, R^R, can be computed by Eq. 1

$$R^R = \hat{H}\hat{H}^H \tag{1}$$

where $(\cdot)^H$ means transponse conjugate.

The Singular Value Decomposition (SVD) described by Eq. 2, provides information about how the possible sub-channels are weighted.

$$R^R = U\Sigma V^H \tag{2}$$

$$\Sigma = \begin{pmatrix} \sigma_1 & 0 & \dots & 0 \\ 0 & \sigma_2 & \dots & 0 \\ \vdots & \vdots & \ddots & \vdots \\ 0 & 0 & \dots & \sigma_i \end{pmatrix} \tag{3}$$

A suitable parameter to evaluate the MIMO performance in terms of increment of the maximum theoretical capacity is the

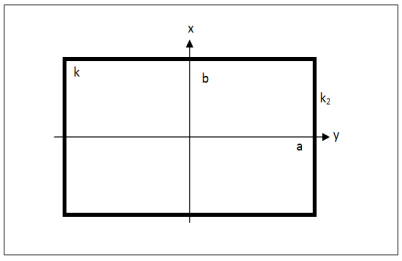

(a)

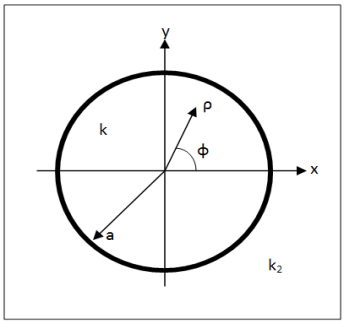

(b)

Fig. 1. Considered tunnels. (a) Rectangular tunnel cross section. (b) Circular tunnel cross section.

Effective Degrees of Freedom (EDOF) parameter [12] defined by the Eq. 4 as the significance of the second eigenvalue of R^R compared with the first one.

$$EDOF = \frac{\sum_{i=1}^{M} min(\sigma_i)}{max(\sigma_i)} \tag{4}$$

This value measure the uncorrelation between the two possible signals for a given channel matrix $\hat{H}$ by its correlation channel matrix at the receiver R^R.

Keeping these definitions in mind, this work is focused on analyzing the influence of the Multi-Element Antenna (MEA) placement and the elements polarization on the EDOF distribution along distance for two canonical cross-section: rectangular and circular.

In section II the authors summarize the method applied to obtain the channel matrix considering a 2x2 MEA inside the tunnel. In section III a brief description of the simulations which have been carried out during the study is provided and the obtained results are commented. In section IV the

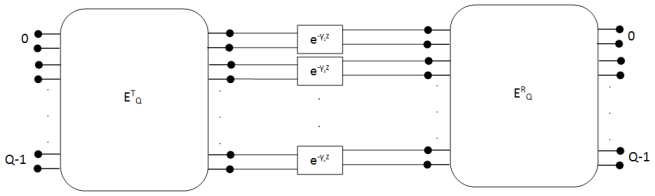

Fig. 2. System block diagram of the applied method to estimate the channel matrix H.

possibilities of the MEA placement and configuration in terms of EDOF improvement are discussed.

II. Channel Matrix Estimation

The method applied to evaluate the impact of the mentioned parameters of the MEA on the EDOF distribution along distance is based on the modal decomposition of the field radiated by the antennas in the tunnel. A brief description of the applied method and the modal computation of the electrical field on the tunnel cross section is presented.

A. Estimation Method

Fig. 2 shows a system block diagram which summarizes the method to estimate the channel matrix $\hat{H}$.

Let us place Q antennas inside the tunnel excited by a certain input current. Let us consider m different relevant modes propagating in the tunnel when it is considered as a dielectric waveguide.

The field in the cross-section of a certain tunnel is given by Eq. 5.

$$\vec{E}(x,y) = \sum_{n=1}^{N} A_n \vec{e_n}(x,y) \tag{5}$$

where A_n are the excitation coefficients of each mode and $\vec{e_n}(x,y)$ the field distribution of the mode. Considering an antenna that produces a $\hat{e}_f(x,y)$ electric field distribution on the tunnel cross section, the A_n values are computed by Eq. 6.

$$A_n = \int\int \vec{e_n}(x,y)\vec{e_f}^*(x,y)dS \tag{6}$$

where $\hat{e}_f(x,y)$ is calculated by the method presented at [10] and the integral is extended over the surface of the cross-section.
Therefore, the channel matrix can be estimated by Eq. 7

$$\bar{H} = \bar{E_Q^T}^H \bar{\gamma} \bar{E_q^R} \tag{7}$$

where $E_Q^{T,R}$ are the coefficient matrices which express the coupling between antennas and modes, at the transmitter (T) and at the receiver (R) and $\bar{\gamma}$ is the diagonal matrix given by Eq. 8.

$$\bar{\gamma} = \begin{pmatrix} e^{-\gamma_1 z} & 0 & \dots & 0 \\ 0 & e^{-\gamma_2 z} & \dots & 0 \\ \vdots & \vdots & \ddots & \vdots \\ 0 & 0 & \dots & e^{-\gamma_k z} \end{pmatrix} \tag{8}$$

B. Modal Analysis inside Tunnels

Fig. 1 shows the cross section of the tunnels that have been considered in this work. For both cases the electric and magnetic field can be expressed by Eq. 9.

$$\begin{aligned} E_z &= e_z e^{-\gamma z} \\ H_z &= h_z e^{-\gamma z} \end{aligned} \tag{9}$$

where γ is the propagation constant with $\gamma = \alpha + j\beta$. The studies presented at [8], [7] and summarized in [9] gives the final expressions of the longitudinal transversal fields for both cases, circular and rectangular tunnel (Eq. 11 and Eq. 12).
If the z-oriented fields inside a circular tunnel are given by Eq. 10.

$$\begin{aligned} E_z &= A cos(\nu\phi) J_\nu(k\rho) e^{\gamma z} \\ H_z &= B sin(\nu\phi) J_\nu(k\rho) e^{\gamma z} \end{aligned} \tag{10}$$

where J_ν is the First Kind Bessel Function, ν is the mode index and $k^2 = \gamma^2 + \omega^2\mu\epsilon$ with ϵ the complex permittivity of the tunnel walls. Then, the transversal electrical and magnetic fields inside circular tunnels are given by Eq. 11.

$$\begin{aligned} E_\phi &= \frac{1}{k^2}[i\omega\mu_0 \frac{\partial}{\partial\rho} H_z - \frac{\gamma}{\rho}\frac{\partial}{\partial\phi} E_z] \\ E_\rho &= \frac{-i\omega\mu 0}{k^2}\frac{1}{\rho}\frac{\partial}{\partial\phi} H_z + \frac{1}{\gamma}[\frac{\omega^2\mu_0\epsilon}{\omega^2\mu_0\epsilon + \gamma^2} - 1]\frac{\partial}{\partial\rho} E_z \end{aligned} \tag{11}$$

Following the approximations presented at [7] the transversal electric field inside a rectangular tunnel is give by Eq. 12.

$$\begin{aligned} E_x^{nm} &= \Big[\frac{sin(\frac{xm\pi}{2a})}{cos(\frac{xm\pi}{2a})}\Big] . \Big[\frac{sin(\frac{yn\pi}{2b})}{cos(\frac{yn\pi}{2b})}\Big] \frac{m, even; n, even}{m, odd; n, odd} \\ E_y^{nm} &= \Big[\frac{sin(\frac{xm\pi}{2a})}{cos(\frac{xm\pi}{2a})}\Big] . \Big[\frac{sin(\frac{yn\pi}{2b})}{cos(\frac{yn\pi}{2b})}\Big] \frac{n, even; m, even}{n, odd; m, odd} \end{aligned} \tag{12}$$

where n and m are the mode index for an hybrid HE_{nm} mode. The complex propagation constant γ is computed by the approximations presented at [9] which provide the complex propagation constants given in Eq. 13 for the circular tunnels and Eq. 14 for the rectangular tunnels.

$$\begin{aligned} \hat{ka}_m^{TE} &= [(ka)_m^{(1)}[1 + \frac{j}{k_0 a(\epsilon - 1)^{\frac{1}{2}}}]] \\ \hat{ka}_{nm}^{HE} &= [[1 + \frac{j(\epsilon + 1)}{2k_0 a(\epsilon - 1)^{\frac{1}{2}}}]] \end{aligned} \tag{13}$$

where $(ka)_m^{(1)}$ is the solution of $J_1(ka) = 0$ and $\hat{ka}_{nm}$ is computed for the HE and TE relevant modes [9].

$$Im(k^x) = -\frac{1}{a}\left(\frac{m\lambda}{4a}\right)^2 Re\left[\frac{\epsilon}{(\epsilon-1)^{\frac{1}{2}}}\right] - \frac{1}{b}\left(\frac{n\lambda}{4b}\right)^2 Re\left[\frac{1}{(\epsilon-1)^{\frac{1}{2}}}\right]$$
$$Re(k^x) = \frac{2\pi}{\lambda}\left[1 - \frac{1}{2}\left(\frac{m\lambda}{4a}\right)^2 - \frac{1}{2}\left(\frac{n\lambda}{4b}\right)^2\right]$$
$$Im(k^y) = -\frac{1}{a}\left(\frac{m\lambda}{4a}\right)^2 Re\left[\frac{1}{(\epsilon-1)^{\frac{1}{2}}}\right] - \frac{1}{b}\left(\frac{n\lambda}{4b}\right)^2 Re\left[\frac{\epsilon}{(\epsilon-1)^{\frac{1}{2}}}\right]$$
$$Re(k^y) = \frac{2\pi}{\lambda}\left[1 - \frac{1}{2}\left(\frac{m\lambda}{4a}\right)^2 - \frac{1}{2}\left(\frac{n\lambda}{4b}\right)^2\right] \quad (14)$$

Fig. 3 shows some examples of the field distributions for the rectangular tunnels computed with the expressions presented above.

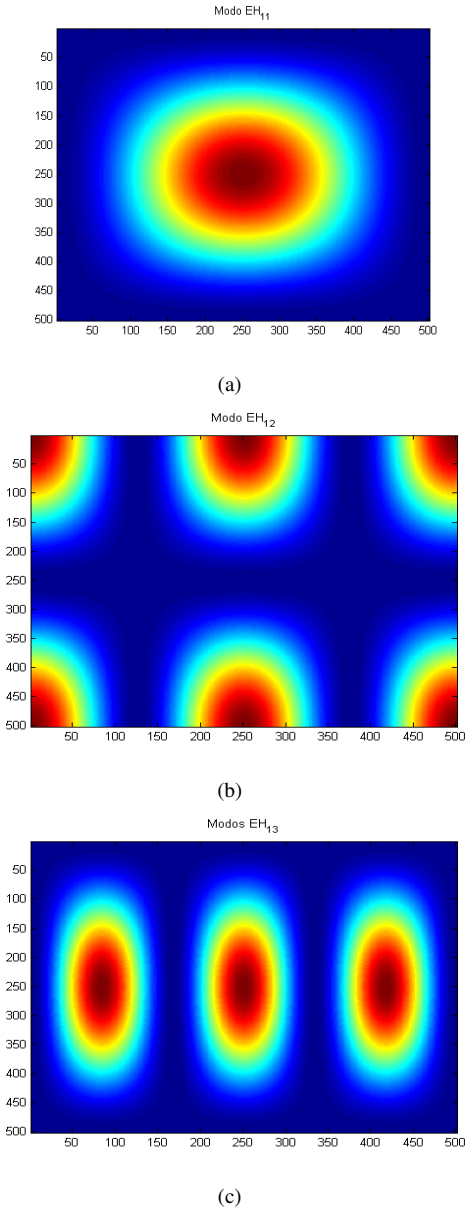

(a)

(b)

(c)

Fig. 3. Examples of the X-polarized electrical field distributions for a rectangular tunnel. (a) EH_{11} mode. (b) EH_{12} mode. (c) EH_{13} mode.

III. EDOF Simulations

In order to evaluate the influence of the MEA placement and polarization on the MIMO performance, the behavior along distance of the EDOF figure of merit defined by Eq. 4 is studied.

The simulations carried out for a circular tunnel are depicted at Fig. 4 where a circular tunnel of $r = 2m$ and $\epsilon = 12$, $\sigma = 0.02\frac{S}{m}$ as an electric constants of the tunnel walls are considered. The simulations carried out for a rectangular tunnel are depicted at Fig. 6 where $2a = 7.8m$ and $2b = 5.3$ and electric constants of $\epsilon = 5$ and $\sigma = 0.01\frac{S}{m}$ are considered.

A. Circular Tunnel Simulations

Inside the circular tunnel described above two infinitesimal dipoles have been considered as transmitting MEA in three different postions with a 6λ antenna spacing and no polarization coupling between elements. The three positions have been proposed in order to simulate the possible placement of a real base station inside the tunnel. These placements are described by their angular parameter as follows:

- pos1: $\Phi_0 = \frac{\pi}{2}$
- pos2: $\Phi_0 = \frac{\pi}{4}$
- pos1: $\Phi_0 = \pi$

where Φ_0 is the angular posistion of the MEA and Φ is defined in the Fig. 1(b).

The receiving MEA has been placed at the center of the tunnel with 6λ antenna spacing and it has been moving along a straight tunnel during 600m simulating the train movement inside the tunnel and the MEA placement on the train. The estimated channel matrix has been computed each meter with two polarization configuration at the transmitting and receiving MEAs simultaniusly, Horizontal-Horizontal (HH) polarization and Vertical-Horizontal (VH) polarization.

Fig. 5 shows the EDOF distribution along distance for the simulations carried out. This EDOF distribution shows the effect of the polarization diversity technique over the MIMO performance of the system which will be translated to a slight increment of the maximum theoretical capacity. This figure also shows the impact of the different positions of the transmitting MEA.

B. Rectangular Tunnel Simulations

In order to compere the EDOF distribution behavior inside different kind of tunnels, the simulations presented at section III-A have been reproduced for the rectangular tunnel described at the beginning of the section III. These experiments are depicted at Fig. 6 and their results are depicted at Fig. 7.

The EDOF distribution along the considered rectangular tunnel shows a smoother behavior than in the circular tunnel. This effect has its origin on the fact that there is a richer set of modes excited by the antennas in a circular tunnel than in the rectangular one where only the hybrid modes are allowed [7].

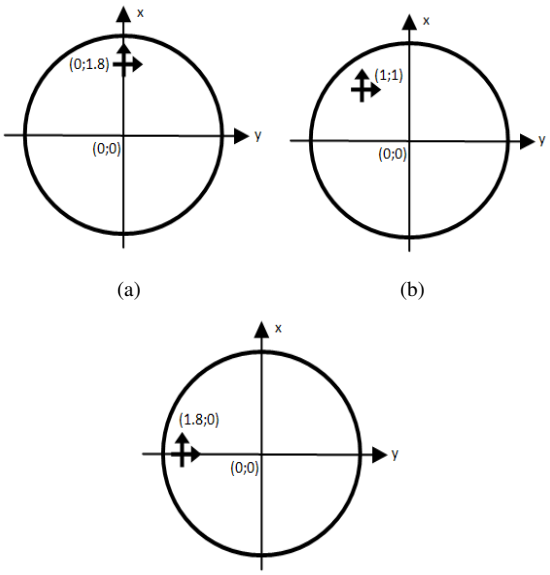

Fig. 4. Experiments to evaluate the impact of the MEA placement and configuration in circular tunnel for a 6λ antenna spacing and real placements of the transmitting and receiving MEA. (a) TX MEA at position pos1 (b) Tx MEA at position pos2. (c) TX MEA at position pos3.

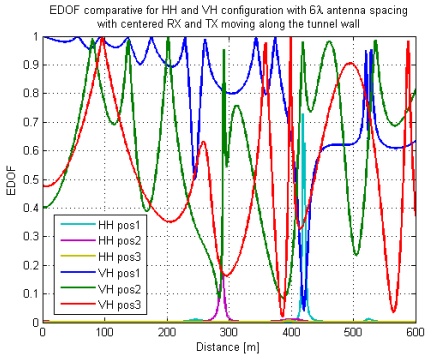

Fig. 5. EDOF distribution along distance for the optimal position of the transmitting MEA with a 6λ antenna spacing and receiving MEA simulating the train position in a circular tunnel.

C. Cross-Polarization Discrimination (XPD) Simulations

The analysis presented at section III-A and III-B leads to conclude that the combination of spatial and polarization diversity is a good method to improve the MIMO performance of a communication system based on MEAs working in subway environments. However recent studies [13] [3] [14] [6] have shown that these diversity techniques provide a low increment on the maximum theoretical capacity when they are applied in a subway and tunnel environments.

The main contributtion on the degradation of the MIMO performance is due to the XPD degradation [3] [15]. In this work, the authors have analyzed the effect of the XPD degradation due to the cross-polar radiation of the antennas in rectangular tunnels.

Let us consider a rectangular tunnel with the same physical

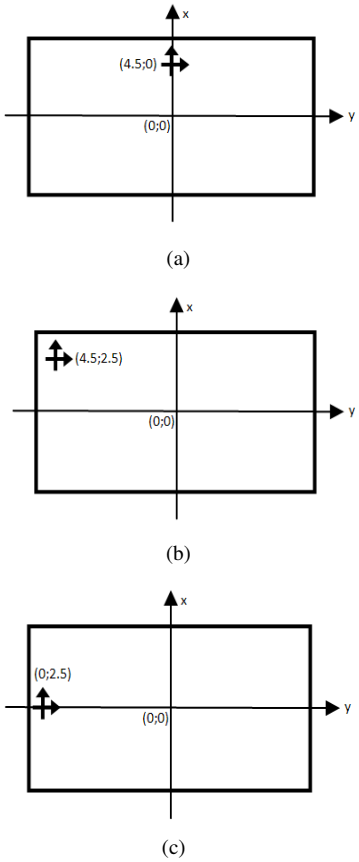

Fig. 6. Experiments to evaluate the impact of the MEA placement and configuration in rectangular tunnel for a 6λ antenna spacing and real placements of the transmitting and receiving MEA. (a) TX MEA at position pos1 (b) Tx MEA at position pos2. (c) TX MEA at position pos3.

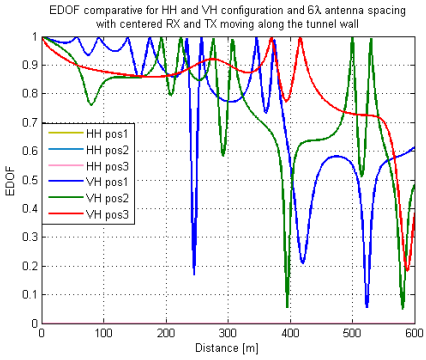

Fig. 7. EDOF distribution along distance for the optimal position of the transmitting MEA with a 6λ antenna spacing and receiving MEA simulating the train position.

characteristics of the tunnel considered at section III-B. Let us consider a transmitting and receiving MEA with a VH configuration and 6λ antenna spacing where an excitation of the cross polarization about 0.1 has been assumed at each element of the MEA (this value produces XPD of 20dB).

Fig. 8 shows the impact on the EDOF distribution along distance of the finite XPD of the transmitting and receiving MEA elements when the same transmitting MEA positions

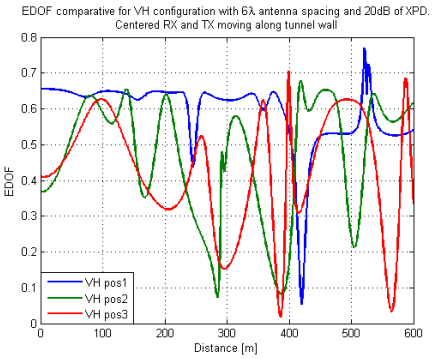

Fig. 8. EDOF distribution along distance for the optimal position of the transmitting MEA with a 6λ antenna spacing and receiving MEA simulating the train position in a circular tunnel. a 20dB XPD is considered at both MEAs

are considered. This figure shows the degradation of the MIMO performance when a finite XPD is considered at the transmitting and receiving MEAs.

IV. Conclusions

In this work a method to study the MIMO performance of a system which works with a MEA as a transmitter and receiver inside tunnels is presented. This method provides information about how the orthogonal modes are excited inside circular and rectangular tunnels and includes the effect of the MEAs positions inside the tunnel and the polarization diversity technique applied on the MIMO performance.
The work also presents the EDOF distribution along distance for several cases of transmitting MEA positions and polarization of both MEAs (TX and RX) when a real scenario is considered (position of the MEAs and finite XPD of the transmitting and receiving MEAs). This cases have lead to conclude that the polarization diversity technique is needed in order to improve the MIMO performance of the system. This is due to the relation between the orthogonal-subchannels generated inside the tunnel by the excitation and the excited 'wave-guide' modes inside it [1] [4].

Acknowledgment

The authors would like to thank Santiago Capdevila for its support and help during the development of this work. S. Capdevila is with the Signal Theory and Communications Department, Universitat Politècnica de Catalunya, Barcelona, Spain. This work was supported in part by the Spanish Interministerial Commission on Science and Technology (CICYT) under projects TEC2007-66698-C04-01/TCM and CONSOLIDER CSD2008-00068 and by the "Ministerio de Educacin y Ciencia" through the FPU fellowship program and IFERCAT (Infraestructures Ferroviàries de Catalunya).

References

[1] S. Loyka, "Multi-antenna capacities of waveguide and cavity channels," *CCECE 2003 - CCGEI 2003, Montreal*, pp. 1509 – 1514, 2003.

[2] M. Lienard, P. Degauque, J. Baudet, and D. Degardin, "Investigation on MIMO channels in subway tunnels," *Selected Areas in Communications, IEEE Journal on*, vol. 21, no. 3, pp. 332–339, 2003.

[3] M. Lienard, A. Nasr, J. M. Garcia-Parco, and P. Degauque, "Experimental analysis of wave depolarization in arched tunnels," *Personal, Indoor and Mobile Radio Communications, 18th Annual IEEE International Symposium on*, 2007.

[4] J. Molina-Garcia-Pardo, M. Lienard, P. Degauque, and L. Dudley, D.G. Juan-Llacer, "Interpretation of mimo channel characteristics in rectangular tunnels from modal theory," *Vehicular Technology, IEEE Transactions on*, vol. 57, pp. 1974 – 1979, 2008.

[5] J. M. Molina-Garcia-Pardo, J. V. Rodriguez, and L. J. Llacer, "Polarized indoor mimo channel measurements at 2.45ghz," *Antennas and Propagation, IEEE Transactions on*, vol. 56, pp. 3818–3828, 2008.

[6] J. Alonso, B. Izquierdo, S. Capdevila, and J. Romeu, "Preliminar propagation and mimo experiments in train tunnels at 5.8ghz," *Antennas and Propagation Society International Symposium, 2009. APSURSI '09. IEEE*, pp. 1–4, 2009.

[7] K. Laakmann and W. Steier, "Waveguides: Characteristics modes of hollow rectangular dielectric waveguides," *Applied Optics*, vol. 15, pp. 1334–1340, 1976.

[8] C. L. Holloway, D. A. Hill, R. A. Dalke, and G. A. Hufford, "Radio wave propagation characteristics in lossy circular waveguides such as tunnels, mine shafts and boreholes," *Antennas and Propagation, IEEE Transactions on*, vol. 48, NO. 9, pp. 1354–1366, 2000.

[9] D. Dudley, M. Lienard, S. Mahmoud, and P. Degauque, "Wireless propagation in tunnels," *Antennas and Propagation Magazine, IEEE*, vol. 49, no. 2, pp. 11–26, 2007.

[10] J. Rius, A. Lozano, L. Jofre, and A. Cardama, "Spectral propagation algorithm for rcs of perfectly conducting cavities," Jul 1992, pp. 945–948 vol.2.

[11] ——, "Spectral iterative algorithm for rcs computation in electrically large or intermediate perfectly conducting cavities," *Antennas and Propagation, IEEE Transactions on*, vol. 42, no. 6, pp. 790–797, 1994.

[12] F. De Flavis, L. Jofre, J. Romeu, and A. Grau, *Multi-Antenna Systems for MIMO Communications*, C. A. Balanis, Ed. Morgan&ClayPool, 2008.

[13] M. Boutin, A. Benzakour, C. Despins, and S. Affes, "Characterization and Modeling of a Wireless Channel at 2.4 and 5.8 GHz in Underground Tunnels," in *Wireless Communication Systems, 2006. ISWCS '06. 3rd International Symposium on*, A. Benzakour, Ed., 2006, pp. 517–521.

[14] J. Molina-Garcia-Pardo, M. Lienard, P. Degauque, and L. Juan-Llacer, "On mimo channel capacity in tunnels," *Antennas and Propagation, IEEE Transactions on*, vol. 57, pp. 3697 – 3701, 2009.

[15] J. Molina-Garcia-Pardo, M. Lienard, A. Nasr, and P. Degauque, "On the possibility of interpreting field variations and polarization in arched tunnels using a model for propagation in rectangular or circular tunnels," *Antennas and Propagation, IEEE Transactions on*, vol. 56, no. 4, pp. 1206–1211, April 2008.